Cleavage of the BMP-4 Antagonist Chordin by Zebrafish Tolloid

Patrick Blader,* Sepand Rastegar,* Nadine Fischer, Uwe Strähle†

Dorsoventral patterning of vertebrate and *Drosophila* embryos requires bone morphogenetic proteins (BMPs) and antagonists of BMP activity. The *Drosophila* gene *tolloid* encodes a metalloprotease similar to BMP-1 that interacts genetically with *decapentaplegic*, the *Drosophila* homolog of vertebrate BMP-2/4. Zebrafish embryos overexpressing a zebrafish homolog of *tolloid* were shown to resemble loss-of-function mutations in *chordino*, the zebrafish homolog of the *Xenopus* BMP-4 antagonist Chordin. Furthermore, Chordin was degraded by COS cells expressing Tolloid. These data suggest that Tolloid antagonizes Chordin activity by proteolytically cleaving Chordin. A conserved function for zebrafish and *Drosophila* Tolloid during embryogenesis is proposed.

The establishment of pattern during embryogenesis requires an extensive hierarchy of cell-cell signaling (*1*). The activity of members of the BMP family is implicated in ventral cell fate determination in vertebrates. Whereas overexpression of BMP-4 results in an expansion of ventral tissues such as blood and pronephros at the expense of dorsal tissues like notochord and somites (*2–5*), injection of a dominant negative BMP receptor blocks BMP signaling and dorsalizes *Xenopus* and zebrafish embryos (*4–6*). Conversely, the *Xenopus* genes *chordin* and *noggin* are expressed in the organizer and have been implicated in the establishment of dorsal cell fates (*7, 8*). Chordin and Noggin bind directly to BMP-4, thereby blocking interaction with the BMP receptor—suggesting that dorsoventral patterning of the vertebrate embryo is partially accomplished through the antagonism of ventralizing BMP signals (*9, 10*). In agreement, mutations in the gene encoding the zebrafish Chordin homolog *chordino* ventralize zebrafish embryos (*3, 5, 11*).

A similar antagonistic relation is required for the establishment of dorsoventral pattern in the *Drosophila* embryo between *decapentaplegic* (*dpp*) and *short gastrulation* (*sog*) (*12*), which encode the *Drosophila* homologs of vertebrate BMP-2/4 and Chordin, respectively (*13*). Genetic analysis has revealed five other zygotically active genes that appear to be required for this process (*14*). One such gene, *tolloid*, encodes a member of the astacin family of metalloproteases similar to BMP-1 that appears to enhance the activity of *dpp* (*12, 15–17*). However, BMP-1 is identical to the enzyme procollagen C–protease (*18*). It thus remains unclear if vertebrate homologs of *Drosophila* Tolloid have orthologous patterning functions during development and, if so, how they might interact with members of the BMP family to enhance their activities during embryogenesis and bone formation.

We isolated a zebrafish member of the astacin metalloprotease gene family that we named *tolloid* (*tld*), because it shares high homology with *Drosophila* and mammalian Tolloid (*13, 19, 20*) (Fig. 1A). Consistent with an early function for the gene, *tld* transcripts are detected throughout the early gastrula stage embryo (*21, 22*). Toward the end of gastrulation expression becomes restricted, accumulating both dorsally and ventrally around the closing blastopore (Fig. 1B). Expression is also detected in the ectoderm flanking the anterior neural plate at this stage (Fig. 1, B and C). At the 10-somite stage *tld* mRNA is expressed in the developing tailbud and in cells flanking the midbrain and hindbrain that presumably correspond to migrating cranial neural crest (Fig. 1D).

To assay possible functions of zebrafish Tolloid (Tld), we injected synthetic *tld* mRNA into zebrafish embryos (*23*) (Fig. 2 and Table 1). Morphological differences between *tld*-injected embryos and control siblings first become evident at the beginning of somitogenesis when injected embryos display a broader and flatter tailbud (Fig. 2, A and D). At 24 hours, injected embryos are characterized by an expanded yolk extension, disrupted tail development, and an increase in hematopoietic cells (Fig. 2, B and E); head and eyes are smaller in injected embryos. After 48 hours of development, injected em-

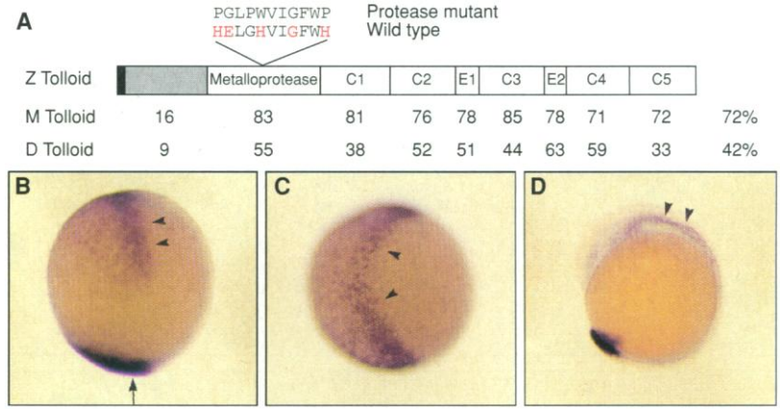

Fig. 1. Predicted protein structure and expression pattern of zebrafish *tld*. (**A**) Schematic representation of zebrafish Tolloid showing the relative organization of the metalloprotease, CUB (C1 to C5) and EGF (E1 and 2) domains; the signal sequence is indicated in black, and a region of unknown function NH_2-terminal to the metalloprotease domain is indicated in gray. Numbers beneath the various domains indicate the percentage amino acid identity between zebrafish (Z), murine (M), and *Drosophila* (D) Tolloid within these domains. The overall amino acid identity between the proteins is indicated at right. Letters above the schematic zebrafish Tolloid represent the wild-type and the protease mutant amino acid sequence in the zinc-binding region of the metalloprotease domain; amino acids in red are thought to be essential for zinc binding (*16*). Abbreviations for the amino acid residues are as follows: E, Glu; F, Phe; G, Gly; H, His; I, Ile; L, Leu; P, Pro; V, Val; and W, Trp. (**B** and **C**) Ninety-five to 100% epiboly stage embryos hybridized with an antisense RNA to *tld*. At the vegetal pole, *tld* expression is localized to the region surrounding the closing blastopore (arrow) with greater expression evident ventrally than dorsally. At the animal pole, *tld* expression is detected flanking the anlage of the anterior neural plate (arrowheads). (**D**) Embryos at the 10-somite stage hybridized with an antisense RNA to *tld*. Strong expression is detected in the tailbud, and weaker expression is detected anteriorly in the cranial neural crest (arrowheads). Expression in the tailbud and neural crest persists until later stages when expression is also detected in cells of the hematopoietic system (*22*). Embryos are viewed animal pole up, dorsal right (B), from the animal pole with dorsal right (C), and anterior up, dorsal right (D).

Institut de Génétique et de Biologie Moléculaire et Cellulaire (IGBMC), CNRS/INSERM/ULP, BP 163, 67404 Illkirch Cedex, C.U. de Strasbourg, France.

*These authors contributed equally to this work.
†To whom correspondence should be addressed. E-mail: uwe@titus.u-strasbg.fr

bryos are generally retarded relative to uninjected controls (Fig. 2, C and F). The increase in the size of the yolk extension is still apparent at this stage as is the expansion of the hematopoietic lineage, and the ventral tail fin is bifurcated (Fig. 2, C and F).

The *eve1* gene is expressed in ventrolateral cells of zebrafish gastrulae (*24*) (Fig. 2, G and I). Expression of *eve1* is expanded dorsally at midgastrulation stages in *tld*-injected embryos (Fig. 2, G to J). The expansion of the hematopoietic lineage at 24 hours in injected embryos is anticipated by an increase in the expression of *gata1*, an early marker of presumptive blood cells (*25*) (Fig. 2, K and L). Furthermore, the expression of *Pax2/pax[zf-b]*, a marker of the ventrally derived pronephros, is also expanded after *tld* injection (*22*, *26*). The morphological and molecular phenotype of *tld*-injected embryos is similar to those caused by injection of low concentrations of BMP-4 mRNA and characteristic of embryos homozygous for the ventralizing mutation *chordino*, except that *chordino* embryos frequently display disruption of the notochord posteriorly, which was not detected in *tld*-injected embryos (*3*, *5*, *11*).

Strong antimorphic alleles of *Drosophila tolloid* carry mutations that map to the metalloprotease domain, whereas nonsense mutations resulting in truncation of *Drosophila* Tolloid immediately COOH-terminal to the metalloprotease domain act as strong null alleles (*27*). Consistent with a conserved function for zebrafish Tld, overexpression of mRNA encoding a Tld mutated in the zinc-binding motif of its metalloprotease domain, Tld^{Mut}, acts antimorphically, resulting in a low frequency of dorsalization (Fig. 1A and Table 1) (*22*). Zebrafish embryos overexpressing a truncated zebrafish Tld, $Tld^{Metallo}$, develop indistinguishably from wild-type siblings showing that, as in *Drosophila*, the complement-Uegf-BMP-1 (CUB) and epidermal growth factor (EGF) domains are required for function of zebrafish Tld (Table 1).

To examine at what level Tld acts in the ventralization pathway, we coexpressed Tld and dorsalizing proteins. Overexpression of a truncated BMP receptor effectively blocked BMP signaling and produced phenotypes similar to those of several recently isolated dorsalizing zebrafish mutations (*4*, *5*, *28*) (Table 1). Embryos injected with both truncated BMP receptor (DN-BR) and *tld* mRNAs were phenotypically identical to embryos injected with DN-BR alone, even at a concentration of *tld* in excess of that needed to produce ventralized embryos (Table 1). Overexpression of *noggin* (*nog*) or *chordin* (*chd*) dorsalizes *Xenopus* embryos by antagonizing the interaction between the ventralizing signal BMP-4 and its receptor (*9*, *10*), a phenotype also seen by overexpression of these proteins in zebrafish embryos (Table 1). Similar to results with DN-BR, *nog/tld*-coinjected embryos were phenotypically indistinguishable from embryos injected with *nog* alone. In contrast, coinjection of a twofold excess of *tld* mRNA with *chordin* mRNA resulted in a significant decrease in the percentage of dorsalized embryos and a concomitant increase in the percentage of ventralized embryos (Fig. 2, E and F, and Table 1). Increasing the concentration of *tld* mRNA

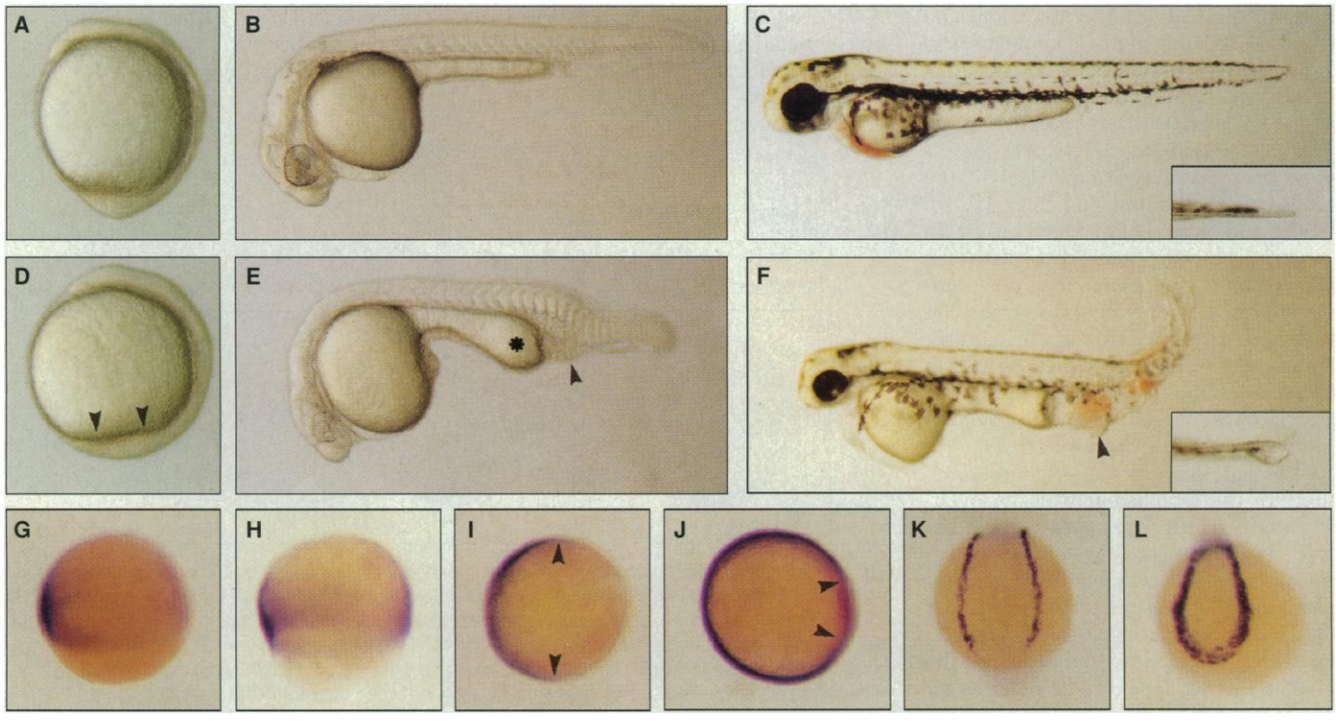

Fig. 2. The morphological and molecular phenotypes of embryos injected with synthetic *tld* mRNA. Uninjected control (**A** to **C**) and *tld*-injected embryos (**D** to **F**); stages are 1-somite (A and D), 24 hours (B and E), and 48 hours (C and F). Embryos injected with synthetic *tld* mRNA display a broader and flatter tailbud at the 1-somite stage (arrowheads in D). At 24 hours, injected embryos are characterized by an expanded yolk extension (asterisk in E), disruption of tail development, and an increase in the size of the pool of hematopoietic cells (arrowhead in E). After 48 hours, the increase in the size of the yolk extension is still apparent as is the expansion of the hematopoietic lineage (arrowhead in F). Also seen at this stage is a bifurcation of the ventral tail fin (compare insets in C and F). Uninjected control (**G**, **I**, and **K**) and *tld*-injected embryos (**H**, **J**, and **L**) at 70% epiboly (G to J) and 12-somite (K and L) stages showing the expression pattern of *eve1* (G to J) and *gata1* (K and L). The ventral marker *eve1* is expanded dorsally at 70% epiboly in injected embryos relative to uninjected controls; arrowheads in (I) and (J) mark the boundary between *eve1*-expressing and -nonexpressing cells. The expansion of the hematopoietic lineage seen morphologically at 24 and 48 hours in injected embryos is anticipated by an increase in the expression of *gata1*, an early marker of presumptive hemopoietic cells. Embryos are viewed animal pole up, dorsal right (A, D, G, and H), anterior left, dorsal up (B, C, E, and F), and in animal view, dorsal right (I and J); embryos are viewed ventrally onto the tailbud, dorsal up (K and L), and insets in (C) and (F) are viewed from the dorsal aspect.

to a fourfold excess almost completely antagonized the dorsalizing effect of *chd* (Table 1). These results suggest that Tld acts at a level above the reception of the BMP signal. Furthermore, because Noggin and Chordin function similarly at the biochemical level (*9*, *10*), these data suggest a specific antagonism of Chordin by Tld.

The homology between zebrafish Tld and procollagen C–protease on the one hand and Chordin and procollagen on the other suggested that in the coinjection experiments, zebrafish Tld might function to antagonize Chordin function by proteolytically cleaving Chordin (*7*, *16*). To test this hypothesis, we examined COS cells overexpressing zebrafish Tld or Tld^{Mut} for their ability to cleave Chordin (*29*) (Fig. 3). Epitope-tagged *Xenopus* Chordin (Chd-MYC) (Fig. 3, lane 1) was unaffected by incubation with mock-transfected COS cells (lanes 2 to 5). Chd-MYC was, likewise, unaffected by incubations with COS cells transfected with Tld^{Mut} (lanes 10 to 13). Conversely, COS cells expressing wild-type Tld progressively degraded Chd-MYC (lanes 6 to 9). Specificity of the affect of Tolloid on Chd-MYC was demonstrated because a second exogenously added protein (RXRα-LBD) was unaffected by incubation with COS cells alone or COS cells transfected with either Tolloid construct.

The results of the transfection experiments are consistent with the ability of *tld* overexpression to phenocopy loss-of-function mutations in *chordino* and with the relation between *tld* and *chd* as determined by coinjection. We propose that overexpression of Tld ventralizes the zebrafish embryo by releasing BMP-2/4–like proteins from inactive complexes with Chordin through proteolytic cleavage of Chordin. The expression of zebrafish *tld* during gastrulation argues for a similar function for endogenous Tld in establishing dorsoventral pattern in the zebrafish embryo. In light of the relation between *Drosophila tld*, *dpp*, and *sog* and their protein homologies with Tld, BMP-2/4, and Chordin, respectively, we suggest that this function has been conserved during vertebrate and invertebrate evolution.

Table 1. Percentages of phenotypes observed after injection of synthetic mRNAs.

Injected material (pg)	*n*	One to three somites	24 hours		
		Dorsalized*	Strong† dorsalized	Weak‡ dorsalized	Ventralized§
tolloid (*tld*) (100)	564	0	0	0	95.2
tolloid^{Mut} (100)	267	4.5	1.9	4.8	0
tolloid^{Metallo} (100)	237	0	0	0	0
DN-BR (100)	179	87.1	83.2	3.3	0
DN-BR/*tld* (100/200)	197	91.4	82.2	7.1	0
noggin (*nog*; 20)	214	92.5	92.5	1.5	0
nog/*tld* (20/200)	233	93.1	92.3	3.8	0
chordin (*chd*; 100)	325	91.7	80.9	8.9	0
chd/*tld* (50/100)	187	22.4	8.0	17.6	29.4
chd/*tld* (50/200)	194	7.2	5.6	5.1	86.1

*As characterized by the rugby-ball shape, expanded notochord, and somites of dorsalized zebrafish mutants (*27*). †Judged to be equal to or more severe than the phenotype of the zebrafish *snailhouse* mutation (*27*). ‡Judged to be equal to or less severe than the phenotype of the zebrafish *piggytail* mutation (*27*). §As characterized by expanded hematopoietic region and yolk extension similar to the ventralizing mutations *chordino* and *mercedes* (*3*, *5*, *11*).

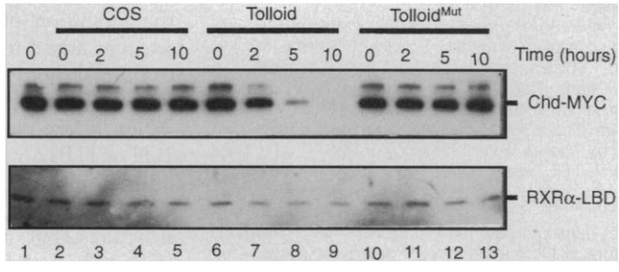

Fig. 3. Chordin is cleaved by COS cells expressing wild-type but not mutated zebrafish Tolloid. Immunoblot analysis of culture media from transfected COS cells (lanes 6 to 13) or mock-transfected COS cells (lane 2 to 5) incubated with c-Myc epitope-tagged Chd and purified retinoid X receptor α–ligand binding domain (RXRα-LBD); lane 1 indicates the presence of anti–c-Myc and anti–RXRα-LBD immunoreactivity in the substrate mix before they were added to the transfected cells. Chd-MYC is cleaved after incubation with cells transfected with a construct expressing wild-type Tolloid (compare lane 6 with lanes 8 and 9) but not with cells expressing a form of Tolloid mutated in the zinc-binding domain (Tolloid^{Mut}, lanes 10 to 13) or mock-transfected COS cells (lanes 2 to 5). RXRα-LBD immunoreactivity is unaffected by incubation with COS cells alone or COS cells transfected with either Tolloid construct.

REFERENCES AND NOTES

1. J. M. W. Slack, *From Egg to Embryo* (Cambridge Univ. Press, Cambridge, UK, 1991); H. L. Sive, *Genes Dev.* **7**, 1 (1993); D. S. Kessler and D. A. Melton, *Science* **266**, 596 (1994).
2. L. Dale, G. Howes, B. M. L. Price, J. C. Smith, *Development* **115**, 573 (1992).
3. M. Hammerschmidt *et al.*, *ibid.* **123**, 95 (1996).
4. B. Neave, N. Holder, R. Patient, *Mech. Dev.* **62**, 183 (1997).
5. M. Hammerschmidt, G. N. Serbedzija, A. P. McMahon, *Genes Dev.* **10**, 2452 (1996).
6. J. M. Graff, R. S. Thies, J. J. Song, A. J. Celeste, D. A. Melton, *Cell* **79**, 169 (1994).
7. Y. Sasai *et al.*, *ibid.*, p. 779.
8. W. C. Smith and R. M. Harland, *ibid.* **70**, 829 (1992).
9. S. Piccolo, Y. Sasai, B. Lu, E. M. De Robertis, *ibid.* **86**, 589 (1996).
10. L. B. Zimmerman, J. M. De Jesus-Escobar, R. M. Harland, *ibid.*, p. 599.
11. S. Schulte-Merker, K. J. Lee, A. P. McMahon, M. Hammerschmidt, *Nature* **387**, 862 (1997).
12. E. L. Ferguson and K. V. Anderson, *Development* **114**, 583 (1992).
13. R. W. Padgett, R. D. St. Johnson, W. M. Gelbart, *Nature* **325**, 81 (1987); R. W. Padgett, J. M. Wozney, W. M. Gelbart, *Proc. Natl. Acad. Sci. U.S.A.* **90**, 2905 (1993); S. A. Holley *et al.*, *Nature* **376**, 249 (1995); V. François and E. Bier, *Cell* **80**, 19 (1995).
14. G. Jurgens, E. Wieschaus, C. Nüsslein-Volhard, H. Kluding, *Wilhelm Roux's Arch. Dev. Biol.* **193**, 283 (1984); C. Nüsslein-Volhard, E. Wieschaus, H. Kluding, *ibid.*, p. 267; B. T. Wakimoto, R. F. Turner, T. C. Kaufman, *Dev. Biol.* **102**, 147 (1984); E. Wieschaus, C. Nüsslein-Volhard, G. Jurgens, *Wilhelm Roux's Arch. Dev. Biol.* **193**, 296 (1984); S. B. Zusman and E. Wieschaus, *Dev. Biol.* **111**, 359 (1985).
15. M. J. Shimell, E. L. Ferguson, S. R. Childs, M. B. O'Connor, *Cell* **67**, 469 (1991).
16. M. P. Sarras Jr., *BioEssays* **18**, 439 (1996).
17. J. M. Wozney *et al.*, *Science* **242**, 1528 (1988).
18. S.-W. Li *et al.*, *Proc. Natl. Acad. Sci. U.S.A.* **93**, 5127 (1996); E. Kessler, K. Takahara, L. Biniaminov, M. Brusel, D. S. Greenspan, *Science* **271**, 360 (1996).
19. K. Takahara, G. E. Lyons, D. S. Greenspan, *J. Biol. Chem.* **269**, 32572 (1994); M. Fukagawa, N. Suzuki, B. L. M. Hogan, C. M. Jones, *Dev. Biol.* **163**, 175 (1994).
20. A partial cDNA fragment encoding part of the metalloprotease domain of a zebrafish Tolloid homolog was isolated by reverse transcriptase–polymerase chain reaction (RT-PCR) with RNA from 24-hour embryos as template and the following oligonucleotide primers: GCTACCAGAATTCGCIATGIGICA(C/T)TGGGA and AGTACGGGATCCITTICIIGC(A/G)TA(A/G)TGCAT. The PCR fragment was used as a probe against a gastrula stage cDNA library, and several positive phage were purified and their inserts liberated by in vitro excision. The plasmid with the largest cDNA insert (GenBank accession number AF027596) was sequenced on both strands.
21. In situ hybridization with digoxygenin-incorporated antisense RNA probes was done as decribed [E. Oxtoby and T. Jowett, *Nucleic Acids Res.* **21**, 1087 (1993)]. Fish embryo raising and staging were as described [M. Westerfield, *The Zebrafish Book* (Univ. of Oregon Press, Eugene, 1995)].
22. P. Blader, S. Rastegar, N. Fischer, U. Strähle, data not shown.
23. Wild-type and mutated zebrafish *tolloid* injection constructs were generated by PCR in two steps with the high-fidelity *Pfu* polymerase (Stratagene) to avoid the introduction of amplification artifacts. DNA encoding a region from the initiation methionine to the end of the metalloprotease domain was amplified and cloned into pCS2+ to generate pCS2:Metallo; the corresponding mutated construct, pCS2:Metal-

lo^{Mut}, was assembled from two PCR fragments in which internal oligonucleotide primers were designed to introduce amino acid substitutions in the resultant zinc-binding domain. Subsequently, a PCR fragment encoding the COOH-terminal portion of zebrafish Tolloid was subcloned into pCS2:Metallo or pCS2:Metallo^{Mut}. The two resultant full-length constructs, pCS2:Tolloid and pCS2:Tolloid^{Mut}, were linearized with Not I and transcribed with the Message Machine Kit (Ambion). For transfection into COS cells, constructs were tagged at the COOH-terminus with the Myc epitope. The integrity of synthetic RNAs was assessed on agarose gels, and the RNAs were diluted in water to their respective final injection concentrations immediately before injection. Synthetic mRNAs were injected into the yolk of one- to two-cell-stage embryos with a gas-driven microinjector (Eppendorf).

24. J. S. Joly, C. Joly, S. Schultemerker, H. Boulekbache, H. Condamine, *Development* **119**, 1261 (1993).
25. H. W. Detrich *et al.*, *Proc. Natl. Acad. Sci. U.S.A.* **92**, 10713 (1995).
26. S. Krauss, T. Johansen, V. Korzh, A. Fjose, *Development* **113**, 1193 (1991); A. W. Püschel, M. Westerfield, G. R. Dressler, *Mech. Dev.* **38**, 197 (1992).
27. A. L. Finelli, C. A. Bossie, T. Xie, R. W. Padgett, *Development* **120**, 861 (1994).
28. M. C. Mullins *et al.*, *ibid.* **123**, 81 (1996).
29. Epitope-tagged Chordin (Chd-MYC) was produced from a baculovirus construct with the use of High-Five cells (Invitrogen) (*9*), and Myc immunoreactivity was subsequently monitored by protein immunoblotting with monoclonal antibody to Myc (9E10) [G. L. Evans, G. K. Lewis, G. Ramsey, J. M. Bishop, *Mol. Cell. Biol.* **5**, 3610 (1985)]. Purified retinoid X receptor α–ligand binding domain (RXRα-LBD) was used as a control for protease specificity [W. Bourguet *et al.*, *Protein Express. Purif.* **6**, 604 (1995)]. COS cells were transfected with various DNA constructs with DEAE dextran as described [B. R. Cullen, *Methods Enzymol.* **152**, 684 (1987)]. Expression of the transfected constructs was monitored in parallel by immunohistocytochemistry. The proteolytic potential of the transfected cells was assayed after 48 hours in culture by removing half of the growth media from the COS cells and replacing it with an equal volume of prewarmed baculovirus extract supplemented with RXRα-LBD. Samples of the resulting media were removed at various times after addition of the substrates and were assayed for immunoreactivity by protein immunoblotting. Proteins from the transfected constructs were expressed at a level insufficient for detection by protein immunoblotting of the COS supernatants.

30. We are indebted to H.-F. Kung for providing the DN-BR expression construct, R. Harland for providing the *Xenopus noggin* expression construct, E. M. De Robertis for providing the *Xenopus* Chordin expression plasmid and Chd-MYC–expressing baculovirus, P. Egea for providing the purified RXRα-LBD and anti-RXRα-LBD, and J. S. Joly, S. Krauss, and L. Zon for probes. We thank the staff of the fish and cell culture facilities, the photographers, the oligosynthesis and sequencing groups of the IGBMC, and N. Foulkes for technical assistance and critical reading of the manuscript. P.B. was supported by a Training and Mobility for Researchers (TMR) fellowship from the European Community. U.S. was the recipient of a fellowship from the Deutsche Forschungsgemeinschaft and the Centre International des Etudiants et Stagaires (CIES). Supported by the Institut National de la Santé et de la Recherche Médicale, the Centre National de la Recherche Scientifique, the Centre Hospitalier Universitaire Régional, the Association pour la Recherche sur le Cancer (ARC), the Groupement de Recherche et d'Etudes sur les Génomes (GREG), the Association Français coutre les Myopathies (AFM), and La Ligue contre le Cancer.

6 August 1997; accepted 3 November 1997

Role of Inositol 1,4,5-Trisphosphate Receptor in Ventral Signaling in *Xenopus* Embryos

Shoen Kume,*† Akira Muto, Takafumi Inoue, Kei Suga, Hideyuki Okano, Katsuhiko Mikoshiba

The inositol 1,4,5-trisphosphate (IP_3) receptor is a calcium ion channel involved in the release of free Ca^{2+} from intracellular stores. For analysis of the role of IP_3-induced Ca^{2+} release (IICR) on patterning of the embryonic body, monoclonal antibodies that inhibit IICR were produced. Injection of these blocking antibodies into the ventral part of early *Xenopus* embryos induced modest dorsal differentiation. A close correlation between IICR blocking potencies and ectopic dorsal axis induction frequency suggests that an active IP_3-Ca^{2+} signal may participate in the modulation of ventral differentiation.

In development, the formation of the body plan involves receptor-mediated signal transduction in processes such as mesoderm and neural induction. Activation of the polyphosphoinositide (PI) cycle results in the hydrolysis of phosphatidylinositol 4,5-bisphosphate, producing IP_3 and diacylglycerol (*1*). IP_3 triggers the release of Ca^{2+} from the endoplasmic reticulum into the cytosol through the IP_3 receptor (IP3R) (*2*). The PI cycle has been postulated to function in dorso-ventral (D-V) axis formation in many species, as indicated by the action of lithium (*3*, *4*). Lithium is assumed to block the recycling of IP_3 into inositol by inhibiting the hydrolysis of intermediate inositol phosphates (*3*). Application of lithium to cleavage-stage embryos of *Xenopus laevis* induces dorsalization by conversion of ventral mesoderm to dorsal mesoderm, with a concomitant reduction in posterior structures (*4*). Although some studies suggest that IP_3 functions in transducing ventral signals during mesoderm induction (*5*), other work does not support the inositol depletion hypothesis for the action of lithium (*6*, *7*).

To determine the role of the PI cycle in patterning the body plan, we isolated monoclonal antibodies (mAbs) to the *Xenopus* IP_3 receptor (XIP3R) (*8*, *9*) and analyzed their effects on D-V specification. Protein immunoblot analysis revealed that mAbs 1G9, 11B12, and 7F11 recognized a single band of the same molecular size as XIP3R (*10*) (Fig. 1A). Antibodies 1G9 and 11B12 inhibited IP_3-induced Ca^{2+} release (IICR) in an in vitro assay (*11*) (Fig. 1B). To confirm the inhibitory activity of the mAbs in vivo, we assessed the effects of the mAbs on early *Xenopus* embryos that overexpressed an exogenous PI-coupled receptor, the type I muscarinic acetylcholine receptor (m1AChR) (*12*, *13*) (Fig. 1C). Although 7F11 did not inhibit IICR in the in vitro Ca^{2+} release assay, all three mAbs had inhibitory activity in vivo. In the presence of mAbs 1G9, 11B12, or 7F11, Ca^{2+} release upon ligand application was 26.9, 10.8, or 58.6%, respectively, of that observed in control embryos.

To examine the role of IICR on axis formation, we injected the blocking antibodies into either ventral or dorsal blastomeres. Ventral injection of 1G9, 11B12, or 7F11 at the four-cell stage (*14*) induced the formation of a secondary dorsal axis, whereas dorsal injection (*15*) of the mAbs or normal mouse immunoglobulin G (IgG) (Fig. 2, A and B) showed no obvious effects. When a low dose (20 ng per embryo) of 1G9 or 11B12, or a higher dose of 7F11 (40 ng per embryo), was applied, the induced axes consisted of ectopic muscle and neural structures, but usually lacked notochords (Fig. 2C). At a higher dose of 1G9 (80 ng per embryo), hyperdorsoanteriorization occurred at the expense of dorsoposterior development (*15*). Dose responses of the mAbs are presented in Fig. 2D. The relative potency of the ectopic axis–inducing activity of the mAbs corresponded to their abil-

S. Kume, Mikoshiba Calciosignal Net Project, Exploratory Research for Advanced Technology (ERATO), Japan Science and Technology Corporation (JST), 2-9-3 Shimo-Meguro, Meguro-ku, Tokyo 153, Japan, and Department of Molecular Neurobiology, Institute of Medical Science, University of Tokyo, 4-6-1 Shirokanedai, Minato-ku, Tokyo 108, Japan.
A. Muto, Mikoshiba Calciosignal Net Project, ERATO, JST, 2-9-3 Shimo-Meguro, Meguro-ku, Tokyo 153, Japan.
T. Inoue and K. Suga, Department of Molecular Neurobiology, Institute of Medical Science, University of Tokyo, 4-6-1 Shirokanedai, Minato-ku, Tokyo 108, Japan.
H. Okano, Department of Neuroanatomy, Biomedical Research Center, Osaka University Medical School, Suita, Osaka 565, Japan, and Core Research for Evolutional Science and Technology (CREST), JST, Suita, Osaka 565, Japan.
K. Mikoshiba, Mikoshiba Calciosignal Net Project, ERATO, JST, 2-9-3 Shimo-Meguro, Meguro-ku, Tokyo 153, Japan; Department of Molecular Neurobiology, Institute of Medical Science, University of Tokyo, 4-6-1 Shirokanedai, Minato-ku, Tokyo 108, Japan; and RIKEN Brain Science Institute, 2-1 Hirosawa, Wako, Saitama 351-01, Japan.

*To whom correspondence should be addressed. E-mail: skume@ims.u-tokyo.ac.jp
†Present address: Mikoshiba Calciosignal Net Project, ERATO, JST, 2-9-3 Shimo-Meguro, Meguro-ku, Tokyo 153, Japan.